Impulsive Radiation from a Horizontal Electric Dipole above an Imperfectly Conducting Surface

Mark C. H. Lam

***Abstract*—Solutions for the impulsive wave fields generated by a horizontal electric dipole situated above an imperfectly conducting surface are derived. The space-time expressions for the reflected wave fields open the door to analysis of their properties in the far-, intermediate-, and near-field regions, and can serve as benchmark for numerical methods employed to wave simulation with applications in antenna design and radio communication. The EM properties of the conductive material are represented by a surface impedance and translated to the wave motion via employing the local plane wave relation as the boundary condition. At the core of tackling the impedance boundary value problem is the derivation of three space-time reflected-wave Green's functions. In contrast to the vertical electric dipole problem, a coupling term is present in the transform-domain wave solutions, and hinders direct application of the extended Cagniard-de Hoop method. A partial-fraction decomposition of this coupling term is the key to furnishing the transformation back to the time domain. Numerical results illustrate time traces and spectra of the measurable reflected electric field strength.**

***Index Terms*—Impedance boundary condition, imperfectly conducting surface, impulsive wave reflection, horizontal electric dipole.**

I. Introduction

The impedance boundary formulation, [1], [2], is useful in EM applications, where wave simulation is performed in geometrically complex-structured configurations characterized by imperfectly conductive materials. The approximating representation of conducting bodies via the surface impedance boundary condition (IBC), e.g. [3], [4], [5], [6], is convenient to avoid a costly fine discretization in unstructured mesh grid modelling methods, such as the finite-element method, e.g. [7]. This applies also to the FDTD method, [8], which in conjunction with the IBC, e.g. [9], [10], has found widespread applications in the modelling of thin conductive structures, e.g. [11], [12], [13], [14]. Applications are found in antenna simulation, micro-strip design, e.g. [15], [16], and on-chip interconnect modelling, e.g. [17], [18], [19].

In this paper, the impulsive radiation from an electric dipole situated above an imperfectly conducting medium, e.g. [20], is studied in the time domain. To this end, the canonical configuration consisting of a planar boundary separating a homogeneous, isotropic and non-conducting medium from a homogeneous, isotropic and imperfectly conducting medium is investigated, e.g. [21]. Studies of perfect dielectric media can be found in e.g. [22], [23], and transient problems are found in e.g. [24], [25], [26]. The employed IBC in this paper represents the conductive material's properties at its surface via the local plane wave relation, and simplifies the two-media wave problem to a half-space problem. The case of a horizonal electric dipole (HED) directed parallel to the impedance boundary is investigated, which completes the problem of an arbitrarily oriented electric dipole above a planar conducting surface since the vertical electric dipole (VED) problem has been investigated in [27].

The objective of this paper is to derive solutions for the impulsive EM wave fields after reflection against a planar impedance wall. It turns out that solving this boundary value problem requires the derivation of three space-time reflected-wave Green's functions (RWGFs). To this end, the Cagniard-de Hoop (CdH) method, e.g. [28], [29], [30], is applied to furnishing the analytical transformation back to the time domain. In contrast to the VED problem studied in [27], a coupling term is part of the Laplace-domain wave field solutions and it has a denominator $\Delta_{\rm Y}\Delta_{\rm Z}$, which hinders direct analytical transformation back to the time domain with the aid of the extended CdH method. A partial-fraction decomposition of this coupling term is presented, which is the key to solving the impedance boundary value problem corresponding to the elementary half-space configuration.

This paper develops an analytical benchmark for numerical methods employed to EM wave simulation with applications in antenna design and radio communication. Illustrative numerical results present time traces and spectra of the measurable reflected electric field strength, which can serve as benchmark results.

II. Problem formulation

The EM wave motion is studied in the homogeneous half-space $\mathcal{D}_1 = \{-\infty < x < \infty, -\infty < y < \infty, 0 < z < \infty\}$, which is characterized by the constant electric permittivity ε_1 and magnetic permeability μ_1. The wave speed is consequently $c_1 = (\varepsilon_1\mu_1)^{-1/2}$. Figure 1 shows the configuration including the nomenclature. The space-time wave fields in $\mathcal{D}_1$ satisfy the Maxwell's equations

$$-\mathrm{curl}\ \mathbf{H} + \varepsilon_1\partial_t\mathbf{E} = -\mathbf{J}^{\rm e}, \quad (1)$$

$$\mathrm{curl}\ \mathbf{E} + \mu_1\partial_t\mathbf{H} = -\mathbf{K}^{\rm e}, \quad (2)$$

in which

$$\{\mathbf{J}^{\rm e}, \mathbf{K}^{\rm e}\}(\mathbf{r}, t) = \{J^{\rm e}, 0\}(t)\delta(\mathbf{r} - \mathbf{r}_{\rm s})\mathbf{i}_x, \quad (3)$$

are the volume density of externally applied electric and magnetic current density, respectively. The symbol $J^{\rm e}$ stands for the source signature, $\delta(\mathbf{r})$ is the Kronecker delta function operative at $\mathbf{r}$, and $\mathbf{r}_{\rm s} = (0, 0, h)$ denotes the position of the

Manuscript received XXXX xx, 2011; revised XXXX xx, XXXX.

Mark C. H. Lam, 23 Jasmijnstraat, 4621 DA, Bergen op Zoom, Noord-Brabant, The Netherlands (e-mail: mark.lam.2008@gmail.com).

point source, with $h \geq 0$ the source height. The source starts to act at $t = 0$ and prior to this time instant the configuration is at rest.

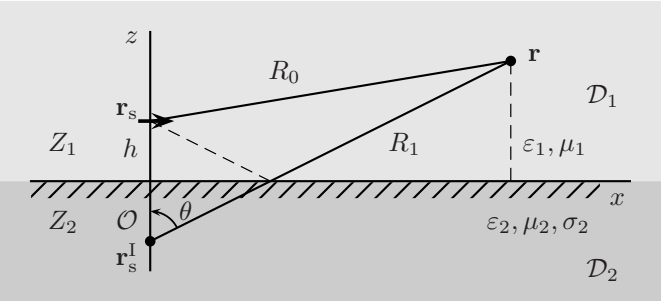

Fig. 1. Elementary configuration consisting of a planar interface $\partial\mathcal{D}$ separating two media. Half-space $\mathcal{D}_1$ is homogeneous, nonconducting and characterized by the wave impedance Z_1, whereas half-space $\mathcal{D}_2$ is homogeneous, conducting and characterized by the wave impedance Z_2. With the surface impedance boundary condition, the electric properties in $\mathcal{D}_2$, called second medium, are represented at $\partial\mathcal{D}$. The symbol $\mathbf{r}_\mathrm{s}$ denotes the dipole source position, $\mathbf{r}_\mathrm{s}^\mathrm{I}$ the image source position, and h the source height. Furthermore, R_0 is the distance between source and receiver, and R_1 is the distance between image source and receiver.

Let $Y_1 = (\varepsilon_1/\mu_1)^{1/2}$ and $Z_1 = (\mu_1/\varepsilon_1)^{1/2}$ denote the wave admittance and wave impedance of $\mathcal{D}_1$, respectively. Furthermore, let $Y_\mathrm{n}(t)$ and $Z_\mathrm{n}(t)$ stand for the specific wave admittance and the specific wave impedance of $\mathcal{D}_2$, respectively. Specific means normalized with respect to its counterpart in $\mathcal{D}_1$. Then, the EM properties of the planar boundary are modelled via the linear, time-invariant, local admittance relation,

$$\mathbf{H}_\mathrm{T}(x,y,0,t) = -Y_2(t) \overset{(t)}{*} [\mathbf{E}_\mathrm{T}(x,y,0,t) \times \mathbf{n}], \quad (4)$$

in which $Y_2(t) = Y_1 Y_\mathrm{n}(t)$ is the wave admittance of $\mathcal{D}_2$, or the local impedance relation

$$\mathbf{E}_\mathrm{T}(x,y,0,t) = -Z_2(t) \overset{(t)}{*} [\mathbf{n} \times \mathbf{H}_\mathrm{T}(x,y,0,t)], \quad (5)$$

in which $Z_2(t) = Z_1 Z_\mathrm{n}(t)$ is the wave impedance of $\mathcal{D}_2$. In these expressions, the operation $\overset{(t)}{*}$ denotes temporal convolution and the subscript T stands for the tangential component. The EM wave field in $\mathcal{D}_1$ is defined as the sum of the incident wave field $\{\mathbf{E}^\mathrm{inc}, \mathbf{H}^\mathrm{inc}\}$, which is the wave field in the absence of the lossy material in $\mathcal{D}_2$, and the reflected wave field $\{\mathbf{E}^\mathrm{ref}, \mathbf{H}^\mathrm{ref}\}$, which expresses the presence of the planar boundary,

$$\{\mathbf{E}, \mathbf{H}\}(\mathbf{r},t) = \{\mathbf{E}^\mathrm{inc}, \mathbf{H}^\mathrm{inc}\}(\mathbf{r},t) + \{\mathbf{E}^\mathrm{ref}, \mathbf{H}^\mathrm{ref}\}(\mathbf{r},t). \quad (6)$$

The focus in the remainder is on the derivation of the space-time reflected EM wave fields in $\mathcal{D}_1$.

The time-invariance and causality of the EM wave fields are taken into account by the use of the unilateral Laplace transform

$$\{\hat{\mathbf{E}}, \hat{\mathbf{H}}\}(\mathbf{r},s) = \int_{t=0}^{\infty} \exp(-st)\{\mathbf{E}, \mathbf{H}\}(\mathbf{r},t)\mathrm{d}t, \quad (7)$$

in which the Laplace transform parameter s is taken positive and real. According to Lerch's theorem [31], a one-to-one mapping exists then between $\{\mathbf{E}, \mathbf{H}\}(\mathbf{r},t)$ and their Laplace transformed counterparts $\{\hat{\mathbf{E}}, \hat{\mathbf{H}}\}(\mathbf{r},s)$. The configuration is initially at rest, so the transform rule $\partial_t \to s$ holds. The complex slowness representation for $\{\hat{\mathbf{E}}, \hat{\mathbf{H}}\}(\mathbf{r},s)$ are introduced as

$$\{\hat{\mathbf{E}}, \hat{\mathbf{H}}\}(\mathbf{r},s) = \frac{s^2}{4\pi^2} \int_{\alpha=-\infty}^{\infty} \mathrm{d}\alpha \int_{\beta=-\infty}^{\infty} \{\tilde{\mathbf{E}}, \tilde{\mathbf{H}}\}(\alpha,\beta,z,s) \exp[-\mathrm{i}s(\alpha x + \beta y)]\mathrm{d}\beta, \quad (8)$$

in which i stands for the imaginary unit, and α and β denote the wave slowness in the x and y directions, respectively. The transform rules $\partial_x \to -\mathrm{i}s\alpha$ and $\partial_y \to -\mathrm{i}s\beta$ apply.

III. Space-time structure of the reflected electromagnetic wave fields

Let $R_1(\mathbf{r}) = [x^2+y^2+(z+h)^2]^{1/2} > 0$ denote the distance between image source and receiver, and $T^\mathrm{ref}(\mathbf{r}) = D_1(\mathbf{r})/c_1$ the arrival time of the reflected wave. Let

$$\left\{\mathcal{G}_\mathrm{Y}^\mathrm{ref}, \mathcal{G}_\mathrm{Z}^\mathrm{ref}, \mathcal{G}_\mathrm{C}^\mathrm{ref}\right\}(\mathbf{r},t) = \left\{G_\mathrm{Y}^\mathrm{ref}, G_\mathrm{Z}^\mathrm{ref}, G_\mathrm{C}^\mathrm{ref}\right\}(\mathbf{r},t) H[t - T^\mathrm{ref}(\mathbf{r})], \quad (9)$$

denote reflected-wave Green's functions, in which $H(t)$ stands for the Heaviside unit step function. With the aid of Eqs. (61)-(62) in Appendix A and the slowness-domain counterparts of Eqs. (68)-(73) in Appendix B, the space-time reflected wave field expressions corresponding to the incidence of a horizontal electric dipole generated spherical wave are found as

$$E_x^\mathrm{ref}(\mathbf{r},t) = -\mu_1^{-1}\partial_t^2 J(t) \overset{(t)}{*} \mathcal{G}_\mathrm{Y}^\mathrm{ref}(\mathbf{r},t) - \varepsilon_1^{-1} J(t) \overset{(t)}{*} \partial_x^2 \mathcal{G}_\mathrm{Z}^\mathrm{ref}(\mathbf{r},t) + \varepsilon_1^{-1} J(t) \overset{(t)}{*} \partial_x^2 \mathcal{G}_\mathrm{C}^\mathrm{ref}(\mathbf{r},t), \quad (10)$$

$$E_y^\mathrm{ref}(\mathbf{r},t) = -\varepsilon_1^{-1} J(t) \overset{(t)}{*} \partial_y\partial_x \mathcal{G}_\mathrm{Z}^\mathrm{ref}(\mathbf{r},t) - \varepsilon_1^{-1} J(t) \overset{(t)}{*} \partial_y\partial_x \mathcal{G}_\mathrm{C}^\mathrm{ref}(\mathbf{r},t), \quad (11)$$

$$E_z^\mathrm{ref}(\mathbf{r},t) = \varepsilon_1^{-1} J(t) \overset{(t)}{*} \partial_x\partial_z \mathcal{G}_\mathrm{Z}^\mathrm{ref}(\mathbf{r},t) - 2\varepsilon_1^{-1} J(t) \overset{(t)}{*} \partial_x\partial_z \mathcal{G}_\mathrm{C}^\mathrm{ref}(\mathbf{r},t) - 2\mu_1 \partial_t^2 J(t) \overset{(t)}{*} \partial_x \int_{z'=z}^{\infty} \mathcal{G}_\mathrm{C}^\mathrm{ref}(x,y,z',t)\mathrm{d}z', \quad (12)$$

$$H_x^\mathrm{ref}(\mathbf{r},t) = -c_1^2 \int_{\tau=0}^{t} J(\tau)\mathrm{d}\tau \overset{(t)}{*} \partial_x\partial_y\partial_z \mathcal{G}_\mathrm{C}^\mathrm{ref}(\mathbf{r},t), \quad (13)$$

$$H_y^\mathrm{ref}(\mathbf{r},t) = \partial_t J(t) \overset{(t)}{*} \partial_z \mathcal{G}_\mathrm{Z}^\mathrm{ref}(\mathbf{r},t) - c_1^2 \int_{\tau=0}^{t} J(\tau)\mathrm{d}\tau \overset{(t)}{*} \partial_y^2\partial_z \mathcal{G}_\mathrm{C}^\mathrm{ref}(\mathbf{r},t), \quad (14)$$

$$H_z^\mathrm{ref}(\mathbf{r},t) = -\partial_t J(t) \overset{(t)}{*} \partial_y \mathcal{G}_\mathrm{Z}^\mathrm{ref}(\mathbf{r},t) - c_1^2 \int_{\tau=0}^{t} J(\tau)\mathrm{d}\tau \overset{(t)}{*} \partial_y^3 \mathcal{G}_\mathrm{C}^\mathrm{ref}(\mathbf{r},t). \quad (15)$$

It is clear that the canonical half-space problem is reduced to finding the space-time RWGFs in Eq. (9), to which end the inverse Laplace transformation of

$$\left\{\hat{\mathcal{G}}_\mathrm{Y}^\mathrm{ref}, \hat{\mathcal{G}}_\mathrm{Z}^\mathrm{ref}, \hat{\mathcal{G}}_\mathrm{C}^\mathrm{ref}\right\}(\mathbf{r},s) = \frac{1}{4\pi^2} \int_{\alpha=-\infty}^{\infty} \mathrm{d}\alpha \int_{\beta=-\infty}^{\infty} \mathrm{d}\beta \left\{\tilde{R}_\mathrm{Y}, \tilde{R}_\mathrm{Z}, \frac{-2}{\Delta_\mathrm{Y}\Delta_\mathrm{Z}}\right\} \frac{\exp\{-s[\mathrm{i}(\alpha x + \beta y) + \gamma D_z]\}}{2\gamma}. \quad (16)$$

is required. Here, the reflection coefficients are given by Eqs. (63)-(64), and the coupling term is defined via Eq. (65) in Appendix A. They depend on the plane wave specific admittance of $\mathcal{D}_2$, which is specified as

$$\hat{Y}_{\rm n}(s) = \hat{X}_{\rm Y}^{1/2}(s) = F\left(1+\tau_{\rm rel}^{-1}s^{-1}\right)^{1/2}, \qquad (17)$$

in which $F = (\varepsilon_2/\varepsilon_1)^{1/2}(\mu_1/\mu_2)^{1/2}$ and $\tau_{\rm rel} = \varepsilon_2/\sigma_2$ stands for the second medium's relaxation time constant. The Laplace-domain plane wave specific impedance function is the inverse of the Laplace-domain plane wave specific admittance function, i.e. $\hat{Z}_{\rm n}(s) = 1/\hat{Y}_{\rm n}(s)$. Finally, a check of correctness of Eqs. (10)-(15) is given in Appendix C, where the case of a perfectly reflecting impedance wall is discussed.

IV. Space-time reflected-wave Green's functions

To furnish the analytical transformation of the slowness-domain expression $\tilde{\mathcal{G}}_{\rm I}^{\rm ref}$, with I = Y, Z or C, given by Eq. (16) back to the time domain, the standard procedures of the CdH method, cf. [28], are invoked. The following transformation is carried out first, $\alpha = -ip\cos(\theta) - q\sin(\theta)$ and $\beta = -ip\sin(\theta) + q\cos(\theta)$. Then, the vertical slowness becomes $\gamma(q,p) = [\Omega(q)^2 - p^2]^{1/2}$, with $\Omega(q) = (c_1^{-2}+q^2)^{1/2}$. Next, the integration path along the imaginary axis of the complex p-plane is replaced by the hyperbolic contour $pr+\gamma(z+h) = \tau$, with $T_1(q) < \tau < \infty$, where $T_1(q) = R_1\Omega(q)$. Finally, the transformation $q = (\tau^2/R_1^2 - c_1^{-2})^{1/2}\sin(\psi)$ is carried out and leads to

$$\hat{\mathcal{G}}_{\rm I}^{\rm ref}(\mathbf{r},s) = \frac{1}{4\pi D_1}\int_{\tau=T^{\rm ref}}^{\infty}\hat{K}_{\rm I}^{\rm ref}(\mathbf{r},\tau,s)\exp(-s\tau){\rm d}\tau, \quad (18)$$

in which the quantity

$$\hat{K}_{\rm I}^{\rm ref}(\mathbf{r},\tau,s) = \frac{2}{\pi}\int_{\psi=0}^{\pi/2}{\rm Re}\left\{\tilde{R}_{\rm I}(\overline{\gamma},s)\right\}{\rm d}\psi, \qquad (19)$$

denotes the reflected-wave kernel function. The symbol $T^{\rm ref} = T_1(0) = R_1/c_1$ and $\overline{\gamma}(\mathbf{r},\tau,\psi)$ stands for the vertical slowness after carrying out the indicated transformations. If the causal time-domain counterpart of $\hat{K}_{\rm I}^{\rm ref}(\mathbf{r},\tau,s)$ is known, then the space-time RWGF can be expressed as

$$\mathcal{G}_{\rm I}^{\rm ref}(\mathbf{r},t) = \frac{1}{4\pi R_1}\int_{\tau=T_1}^{t}L_{\rm I}^{\rm ref}(\mathbf{r},\tau,t-\tau){\rm d}\tau H[t-T^{\rm ref}(\mathbf{r})]. \qquad (20)$$

The calculation of the space-time RWGFs is reduced to finding the space-time reflected-wave kernel functions $L_{\rm I}^{\rm ref}(\mathbf{r},\tau,t)$, for I = Y, Z, C, which are discussed next.

A. Reflected-wave Green's function $\mathcal{G}_{\rm Y}^{\rm ref}$

Substitution of the expression for the reflection coefficient $\tilde{R}_{\rm Y}$ in Eq. (19) yields

$$\hat{L}_{\rm Y}^{\rm ref}(\mathbf{r},\tau,s) = 1 + \frac{2}{\pi}\int_{\psi=0}^{\pi/2}{\rm Re}\left\{\hat{D}_{\rm Y}^{\rm ref}\right\}{\rm d}\psi. \qquad (21)$$

Here,

$$\hat{D}_{\rm Y}^{\rm ref}(\mathbf{r},\tau,s) = \frac{-2\hat{Y}_{\rm n}(s)}{\hat{Y}_{\rm n}(s)+c_1\overline{\gamma}}, \qquad (22)$$

with $c_1\overline{\gamma}(\mathbf{r},\tau) = \Gamma_1(\mathbf{r},\tau) - {\rm i}\Gamma_2(\mathbf{r},\tau)\cos(\psi)$, where $\Gamma_1(\mathbf{r},\tau) = (\tau/T^{\rm ref})\cos(\theta)$ and $\Gamma_2(\mathbf{r},\tau) = [(\tau/T^{\rm ref})^2 - 1]^{1/2}\sin(\theta)$. Evaluation of the ψ-integral with the aid of the following identity

$$\frac{2}{\pi}\int_{\psi=0}^{\pi/2}\frac{A}{A^2+B^2\cos^2(\psi)}{\rm d}\psi = \frac{1}{(A^2+B^2)^{1/2}}, \qquad (23)$$

results in

$$\hat{L}_{\rm Y}^{\rm ref}(\mathbf{r},\tau,s) = 1 - \frac{2\hat{Y}_{\rm n}(s)}{\{[\hat{Y}_{\rm n}(s)+\Gamma_1]^2+\Gamma_2^2\}^{1/2}}. \qquad (24)$$

To recast the term on the r.h.s. to a suitable form, the Schouten-Van der Pol theorem of the unilateral Laplace transform, [32], [33], [34], [35], is employed in conjunction with the following identity from the Laplace transform,

$$\frac{s}{[(s+a)^2+b^2]^{1/2}} = \int_{v=0}^{\infty}\partial_v[\exp(-av)J_0(bv)H(v)]\exp(-sv){\rm d}v, \quad (25)$$

in which the symbol J_0 denotes the Bessel function of the first kind and order zero. The result is

$$\hat{L}_{\rm Y}^{\rm ref}(\mathbf{r},\tau,s) = -1 + 2\int_{v=0}^{\infty}K_{\rm C}^{\rm VMD}(\mathbf{r},\tau,v)\hat{K}_{\rm Y}(v,s){\rm d}v, \quad (26)$$

in which

$$\hat{K}_{\rm Y}(v,s) = \exp\left[-v\hat{Y}_{\rm n}(s)\right], \qquad (27)$$

is a kernel function that contains only the boundary's EM properties via the admittance function, and

$$K_{\rm C}^{\rm VMD}(\mathbf{r},\tau,v) = \exp(-\Gamma_1 v)[\Gamma_1 J_0(\Gamma_2 v) + \Gamma_2 J_1(\Gamma_2 v)]H(v), \qquad (28)$$

is a kernel function that depends only on the configuration. The time-domain counterpart is found as

$$\hat{L}_{\rm Y}^{\rm ref}(\mathbf{r},\tau,t) = -\delta(t) + 2\int_{v=0}^{\infty}K_{\rm C}^{\rm VMD}(\mathbf{r},\tau,v)K_{\rm Y}(v,t){\rm d}v. \qquad (29)$$

The problem is reduced to finding the time-domain counterpart of Eq. (27). The procedures are discussed in Appendix D. After transformation back to the time domain, the space-time RWGF is expressed as

$$\mathcal{G}_{\rm Y}^{\rm ref}(\mathbf{r},t) = \mathcal{G}_{\rm Y}^{\rm ref;R}(\mathbf{r},t) + \mathcal{G}_{\rm Y}^{\rm ref;C}(\mathbf{r},t) + \mathcal{G}_{\rm Y}^{\rm ref;D}(\mathbf{r},t), \quad (30)$$

in which the first term on the r.h.s.,

$$\mathcal{G}_{\rm Y}^{\rm ref;R}(\mathbf{r},t) = \frac{1}{4\pi R_1}H[t-T^{\rm ref}(\mathbf{r})], \qquad (31)$$

denotes the perfectly conducting surface RWGF. The second and third terms on the r.h.s. take into account the deviation from the case $\sigma_2 \to \infty$, with

$$\mathcal{G}_{\rm Y}^{\rm ref;C}(\mathbf{r},t) = \frac{1}{4\pi R_1}H[t-T^{\rm ref}(\mathbf{r})]\times -2F\left[(\Gamma_1^2+\Gamma_2^2)+2\Gamma_1 F+F^2\right]^{-1/2}, \quad (32)$$

the remainder of the constant-admittance RWGF, and

$$\mathcal{G}_{\rm Y}^{\rm ref;D}(\mathbf{r},t) = \frac{1}{4\pi R_1}H[t-T^{\rm ref}(\mathbf{r})]\times \quad (33)$$
$$-2F\int_{\tau=T_1}^{t}\mathrm{d}\tau\int_{v=0}^{\infty}\mathrm{d}v\int_{w=0}^{\infty}\mathrm{d}w\ K_{\rm C}^{\rm VMD}(\mathbf{r},\tau,v)\Psi(v,w)\times$$
$$\exp(-F^2w)\left(\frac{\tau_{\rm rel}^{-1}w}{t-\tau}\right)^{1/2}J_1\left\{2F\left[w(t-\tau)/\tau_{\rm rel}\right]^{1/2}\right\},$$

the part of the total-admittance RWGF that represents the dispersive EM response of the imperfectly conducting material to an incident wave. Note that $\mathcal{G}_{\rm Y}^{\rm ref;D}(\mathbf{r},t)$ requires numerical evaluation of a triple integral, which is of the order similar to the case of applying directly 2D inverse Fourier transformation and then inverse Laplace transformation of the transformed domain wave solution. The integrand in $\mathcal{G}_{\rm Y}^{\rm ref;D}(\mathbf{r},t)$, however, is always (1) real-valued, (2) decaying for increasing v and w, and (3) slowly oscillating for physically interesting time windows of observation, say $t<100\tau_{\rm rel}$. It can be shown, but is omitted here, that transformations exist, which avoid integrating over the essential singularity at $w=0$ and which lead to a relaxed requirement for the number of support points needed to perform the 3D integration.

B. Reflected-wave Green's function $\mathcal{G}_{\rm Z}^{\rm ref}$

Substitution of the expression for the reflection coefficient $\tilde{R}_{\rm Z}$ in Eq. (19) yields

$$\hat{L}_{\rm Z}^{\rm ref}(\mathbf{r},\tau,s)=1+\frac{2}{\pi}\int_{\psi=0}^{\pi/2}\mathrm{Re}\left\{\hat{D}_{\rm Z}^{\rm ref}\right\}\mathrm{d}\psi, \quad (34)$$

in which

$$\hat{D}_{\rm Z}^{\rm ref}(\mathbf{r},\tau,s)=\frac{-2\hat{Z}_{\rm n}(s)}{\hat{Z}_{\rm n}(s)+c_1\overline{\gamma}}=\frac{-2}{1+c_1\overline{\gamma}\hat{Y}_{\rm n}(s)}. \quad (35)$$

The transformation back to the time domain goes along similar lines as outlined in [27]. The derivations are omitted here, and the space-time RWGF is expressed as

$$\mathcal{G}_{\rm Z}^{\rm ref}(\mathbf{r},t)=\mathcal{G}_{\rm Z}^{\rm ref;R}(\mathbf{r},t)+\mathcal{G}_{\rm Z}^{\rm ref;C}(\mathbf{r},t)+\mathcal{G}_{\rm Z}^{\rm ref;D}(\mathbf{r},t), \quad (36)$$

in which the first term on the r.h.s.,

$$\mathcal{G}_{\rm Z}^{\rm ref;R}(\mathbf{r},t)=\frac{1}{4\pi R_1}H[t-T^{\rm ref}(\mathbf{r})], \quad (37)$$

denotes the perfectly conducting surface RWGF. The second and third terms on the r.h.s. take into account the deviation from the case $\sigma_2\to\infty$, with

$$\mathcal{G}_{\rm Z}^{\rm ref;C}(\mathbf{r},t) = \frac{1}{4\pi R_1}H[t-T^{\rm ref}(\mathbf{r})]\times$$
$$-2\left[(\Gamma_1^2+\Gamma_2^2)F^2+2\Gamma_1F+1\right]^{-1/2}, \quad (38)$$

the remainder of the constant-impedance RWGF, and

$$\mathcal{G}_{\rm Z}^{\rm ref;D}(\mathbf{r},t) = \frac{1}{4\pi R_1}H[t-T^{\rm ref}(\mathbf{r})]\times \quad (39)$$
$$2F\int_{\tau=T_1}^{t}\mathrm{d}\tau\int_{v=0}^{\infty}\mathrm{d}v\int_{w=0}^{\infty}\mathrm{d}w\ K_{\rm C}^{\rm VED}(\mathbf{r},\tau,v)\Psi(v,w)\times$$
$$\exp(-F^2w)\left(\frac{\tau_{\rm rel}^{-1}w}{t-\tau}\right)^{1/2}J_1\left\{2F\left[w(t-\tau)/\tau_{\rm rel}\right]^{1/2}\right\},$$

the part of the total-impedance RWGF that represents the dispersive EM response of the imperfectly conducting material to an incident wave. The configurational kernel function $K_{\rm C}^{\rm VED}$ is given by

$$K_{\rm C}^{\rm VED}(\mathbf{r},\tau,v)=\Lambda_3\exp(-\Lambda_1v)J_0(\Lambda_2v)H(v), \quad (40)$$

in which $\Lambda_1(\mathbf{r},\tau)=\Gamma_1/(\Gamma_1^2+\Gamma_2^2)$, $\Lambda_2(\mathbf{r},\tau)=\Gamma_2/(\Gamma_1^2+\Gamma_2^2)$ and $\Lambda_3(\mathbf{r},\tau)=1/(\Gamma_1^2+\Gamma_2^2)^{1/2}$.

C. Reflected-wave Green's function $\mathcal{G}_{\rm C}^{\rm ref}$

Substitution of the coupling term in Eq. (19) yields

$$\hat{L}_{\rm C}^{\rm ref}(\mathbf{r},\tau,s)=\frac{2}{\pi}\int_{\psi=0}^{\pi/2}\mathrm{Re}\left(\frac{-2}{\Delta_{\rm Y}\Delta_{\rm Z}}\right)\mathrm{d}\psi. \quad (41)$$

For further analytical derivations, a partial fraction decomposition of the coupling term is performed, which yields

$$\frac{-2}{\Delta_{\rm Y}\Delta_{\rm Z}}=\hat{H}_{\rm Y}(s)\hat{D}_{\rm Y}^{\rm ref}(\mathbf{r},\tau,s)+\hat{H}_{\rm Z}(s)\hat{D}_{\rm Z}^{\rm ref}(\mathbf{r},\tau,,s), \quad (42)$$

in which $\hat{D}_{\rm Y}^{\rm ref}$ and $\hat{D}_{\rm Z}^{\rm ref}$ are given by Eqs. (22) and (35), respectively, and

$$\hat{H}_{\rm Y}(s) = \left[1-\hat{Y}_{\rm n}^2(s)\right]^{-1}=-\frac{s}{(F^2-1)s+F^2\tau_{\rm rel}^{-1}}, \quad (43)$$
$$\hat{H}_{\rm Z}(s) = \left[1-\hat{Z}_{\rm n}^2(s)\right]^{-1}=\frac{s+\tau_{\rm rel}^{-1}}{(1-F^{-2})s+\tau_{\rm rel}^{-1}}. \quad (44)$$

Using this decomposition and the results from the previous two subsections, the space-time RWGF corresponding to the coupling term is easily found as

$$\mathcal{G}_{\rm C}^{\rm ref}(\mathbf{r},t)=H_{\rm Y}(t)\overset{(t)}{*}\mathcal{W}_{\rm Y}^{\rm ref}(\mathbf{r},t)+H_{\rm Z}(t)\overset{(t)}{*}\mathcal{W}_{\rm Z}^{\rm ref}(\mathbf{r},t), \quad (45)$$

in which

$$\mathcal{W}_{\rm Y}^{\rm ref}(\mathbf{r},t) = \mathcal{G}_{\rm Y}^{\rm ref;C}(\mathbf{r},t)+\mathcal{G}_{\rm Y}^{\rm ref;D}(\mathbf{r},t), \quad (46)$$
$$\mathcal{W}_{\rm Z}^{\rm ref}(\mathbf{r},t) = \mathcal{G}_{\rm Z}^{\rm ref;C}(\mathbf{r},t)+\mathcal{G}_{\rm Z}^{\rm ref;D}(\mathbf{r},t), \quad (47)$$

and $H_{\rm Y}(t)$ and $H_{\rm Z}(t)$ are the time-domain counterparts of Eqs. (43) and (44).

V. Spatial differentiation of the reflected-wave Green's functions

The reflected electric field strength $E_y^{\rm ref}(\mathbf{r},t)$ is computed in the numerical section and requires spatial differentiation of $\mathcal{G}_{\rm Z}^{\rm ref}(\mathbf{r},t)$, $\mathcal{W}_{\rm Y}^{\rm ref}(\mathbf{r},t)$ and $\mathcal{W}_{\rm Z}^{\rm ref}(\mathbf{r},t)$. The computation of the corresponding reflected-wave Green's tensors goes along similar lines as presented in [27], where the procedures of dealing with the differentiation of the discontinuous RWGF $\mathcal{G}_{\rm Z}^{\rm ref}(\mathbf{r},t)$ were discussed. These procedures are omitted here and Appendix E presents the expression for $E_y^{\rm ref}(\mathbf{r},t)$ corresponding to $\mathcal{G}_{\rm Z}^{\rm ref}(\mathbf{r},t)$. The other constituents of $E_y^{\rm ref}(\mathbf{r},t)$ corresponding to $\mathcal{W}_{\rm Y}^{\rm ref}(\mathbf{r},t)$ and $\mathcal{W}_{\rm Z}^{\rm ref}(\mathbf{r},t)$ are obtained in a similar fashion.

VI. Numerical results

Let $\mu_0 = 4\pi \times 10^{-7}$ Hm^{-1} be the constant magnetic permeability in both $\mathcal{D}_1$ and $\mathcal{D}_2$. The wave speed in domain $\mathcal{D}_1$ is in all examples taken $c_1 = c_0 = 299792458$ ms^{-1}, which corresponds to the choice $\varepsilon_1 = \varepsilon_0$, where $\varepsilon_0 = (c_0^2\mu_0)^{-1} = 8.8542 \times 10^{-12}$ Fm^{-1} is the electric permittivity of vacuum. The second medium is in the three presented examples filled by different materials, i.e., metal, water and wet soil. The metal is represented by copper with electric parameters $\varepsilon_2 = \varepsilon_0$ and $\sigma_2 = 5.96 \times 10^7$ Sm^{-1}. The relaxation time of copper is calculated as $\tau_{\rm rel} = \varepsilon_2/\sigma_2 = 1.4856 \times 10^{-19}$ s. Sea water is the second investigated material with electric parameters $\varepsilon_2 = 81\varepsilon_0$ and $\sigma_2 = 4.8$ Sm^{-1}, e.g. [36]. The relaxation time of sea water is $\tau_{\rm rel} = \varepsilon_2/\sigma_2 = 1.50 \times 10^{-10}$ s. Wet soil is the third investigated material with electric parameters $\varepsilon_2 = 20\varepsilon_0$ and $\sigma_2 = 0.1$ Sm^{-1}. The relaxation time of wet soil is $\tau_{\rm rel} = \varepsilon_2/\sigma_2 = 1.7708 \times 10^{-9}$ s.

A source signature J is specified for the computation of the wave field constituents. The source signature is taken

$$J(t) = \begin{cases} 0, & t < 0, \\ \frac{\rm d}{{\rm d}t} W^{(m)}(t), & t \geq 0, \end{cases} \tag{48}$$

in which

$$W^{(m)}(t) = W_0 (t/\tau_{\rm s})^m \exp[-m(t/\tau_{\rm s} - 1)] H(t), \tag{49}$$

is a C^{m-1} power exponential function. The symbol $\tau_{\rm s}$ denotes the source signature's characterization time. The amplitude W_0 is chosen such that the maximum value of J is unity. In the calculation of time traces, m is taken four.

Time traces for the reflected electric field strength $E_y^{\rm ref}(\mathbf{r}, t)$ at the position $(x, y, z) = (\sqrt{2}h, \sqrt{2}h, h)$, with $h = 2c_1\tau_{\rm rel}$, are presented now for three different values of $\tau_{\rm s}$. It is convenient to scale $E_x^{\rm ref}(\mathbf{r}, t)$ to the same order of magnitude as the source signature J for a direct check of correctness. Here, $E_y^{\rm ref}$ is displayed via

$$\mathcal{E}_y^{\rm ref}(\mathbf{r}, t) = (4\pi R_1^3) \times \varepsilon_1 E_x^{\rm ref}(\mathbf{r}, t)/T^{\rm ref}(\mathbf{r}), \tag{50}$$

This scaling yields values close to the amplitude of J, for all $\mathbf{r} \in \mathcal{D}_1$. Note that the scaling factor is independent of t. Figure 2(a)-(c) present modelling results corresponding to (a) $\tau_{\rm s} = 2\tau_{\rm rel}$, (b) $\tau_{\rm s} = 4\tau_{\rm rel}$, and (c) $\tau_{\rm s} = 8\tau_{\rm rel}$, for copper as the second medium. The black and blue lines represent the modelled result for the total-admittance and constant-admittance reflected electric field strength, respectively. Their difference is the dispersive EM response, which is represented by the red line. Figure 2(d)-(f) present the corresponding magnitude spectra, which are normalized with respect to $\max_f |\hat{\mathcal{E}}_y^{\rm ref}(f)|$. Figure 3 presents similar modelling results as in Fig. 2, but now for sea water as the second medium. Figure 4 presents similar modelling results as in Fig. 2, but now for wet soil as the second medium.

Finally, a note of the computation time and coding. The generation of the time traces, i.e. mainly the calculation of the triple integrals in the RWGFs, required about 75 seconds on a Pentium 4 laptop computer. The number of support point was taken $(N_t, N_v, N_w) = (20, 30, 25)$ and the (v, w)-integrals were truncated at $(L_v, L_w) = (5, 4)$. The temporal convolution integrals in Eq. (45) were avoided by acting both $\hat{H}_{\rm Y}(s = {\rm i}\omega)$ and $\hat{H}_{\rm Z}(s = {\rm i}\omega)$ on the frequency-domain source signature $\hat{J}(s = {\rm i}\omega)$ and then taking the inverse Fourier transform to obtain a modified time-domain source signature.

VII. Conclusion

Space-time expressions were derived for the EM wave fields after reflection against an imperfectly conducting surface. The source is an impulsive horizontal electric dipole with orientation parallel to the planar impedance wall. At the core of tackling the canonical impedance boundary value problem was the derivation of three space-time reflected-wave Green's functions. In contrast to the vertical electric dipole problem, the coupling term in the transform-domain wave solutions hindered direct application of the extended CdH method. A splitting of the coupling expression via a partial-fraction decomposition was required for the transformation back to the time domain. Numerical results presented time traces and spectra of the measurable reflected electric field strength.

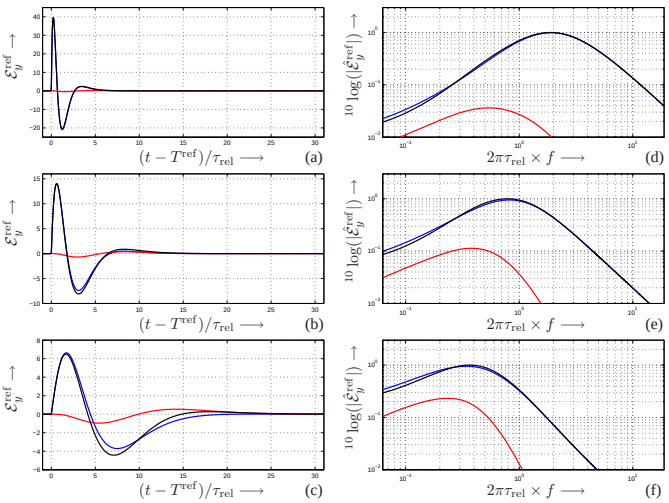

Fig. 2. Copper as the second medium ($\varepsilon_2 = \varepsilon_0$, $\sigma_2 = 5.96 \times 10^7$ Sm^{-1} and $\tau_{\rm rel} = 1.4856 \times 10^{-19}$ s). (a)-(c) Time traces of $\mathcal{E}_y^{\rm ref}(\mathbf{r}, t)$ at the position $(x, y, z) = (\sqrt{2}h, \sqrt{2}h, h)$, with $h = 2\tau_{\rm rel}c_1$. The source signature's characterization time is (a) $\tau_{\rm s} = 2\tau_{\rm rel}$, (b) $\tau_{\rm s} = 4\tau_{\rm rel}$, and (c) $\tau_{\rm s} = 8\tau_{\rm rel}$. (d)-(f) Corresponding normalized magnitude spectrum of $\mathcal{E}_y^{\rm ref}(\mathbf{r}, t)$.

Appendix

A. Slowness-domain reflected wave solutions

The slowness-domain equivalents of Eqs. (1) and (2) are obtained first, and then reduced to second-order equations. This yields the wave equation

$$-\partial_z^2 \tilde{\mathbf{E}} + s^2\gamma^2 \tilde{\mathbf{E}} = -\mu s \hat{\mathbf{J}}^{\rm e} + \frac{1}{\varepsilon s} \tilde{\nabla}(\tilde{\nabla} \cdot \hat{\mathbf{J}}^{\rm e}) - \tilde{\nabla} \times \hat{\mathbf{K}}^{\rm e}, \tag{51}$$

for the electric field strength, and

$$-\partial_z^2 \tilde{\mathbf{H}} + s^2\gamma^2 \tilde{\mathbf{H}} = -\varepsilon s \hat{\mathbf{K}}^{\rm e} + \frac{1}{\mu s} \tilde{\nabla}(\tilde{\nabla} \cdot \hat{\mathbf{K}}^{\rm e}) + \tilde{\nabla} \times \hat{\mathbf{J}}^{\rm e}, \tag{52}$$

for the magnetic field strength. The quantity

$$\gamma(\alpha, \beta) = (c_1^{-2} + \alpha^2 + \beta^2)^{1/2}, \tag{53}$$

denotes the vertical slowness, with ${\rm Re}\{\gamma\} > 0$, and $\tilde{\nabla}$ is the slowness-domain gradient operator. Let $\tilde{\mathcal{G}}^{\rm inc}$ and $\tilde{G}^{\rm ref}$ denote

the transform-domain scalar incident-wave and reflected-wave Green's function, respectively. Then, the solution of the ordinary differential equation

$$-\partial_z^2\tilde{\mathcal{G}}^{\rm inc}+s^2\gamma^2\tilde{\mathcal{G}}^{\rm inc}=\delta(z-h), \tag{54}$$

is useful for solving the half-space problem. After some elaboration, $\tilde{G}^{\rm inc}$ and $\tilde{G}^{\rm ref}$ can be written in the form

$$\left[\begin{array}{c}\tilde{G}^{\rm inc}\\ \tilde{G}^{\rm ref}\end{array}\right](\gamma,z,s)=\left[\begin{array}{c}\tilde{A}^{\rm inc}(\gamma,s)\exp(-s\gamma|z-h|)\\ \tilde{A}^{\rm ref}(\gamma,s)\exp(-s\gamma D_z)\end{array}\right], \tag{55}$$

in which $D_z=z+h$. From Eq. (55), the property $\partial_z\rightarrow\pm s\gamma$ is obtained, which is valid for $z\in(0,h)$. The plus and minus signs correspond to the incident and reflected wave, respectively. Next, a relation between the tangential EM field strengths at the planar surface is derived, for which the following decomposition is convenient,

$$\begin{aligned}\tilde{\mathbf{E}} &= [\tilde{\mathbf{E}}_{\rm T}^T\quad \tilde{E}_z]^T,\ \text{with}\ \tilde{\mathbf{E}}_{\rm T}=[\tilde{E}_x\quad \tilde{E}_y]^T, &(56)\\ \tilde{\mathbf{H}} &= [\tilde{\mathbf{H}}_{\rm T}^T\quad \tilde{H}_z]^T,\ \text{with}\ \tilde{\mathbf{H}}_{\rm T}=[\tilde{H}_x\quad \tilde{H}_y]^T, &(57)\\ \tilde{\nabla} &= [-i s\mathbf{k}_{\rm T}^T\quad \pm s\gamma]^T,\ \text{with}\ \mathbf{k}_{\rm T}=[\alpha\quad \beta]^T. &(58)\end{aligned}$$

The superscript T denotes the vector transpose operation. Application of this decomposition at the slowness-domain equivalents of Eqs. (1) and (2), the following relations can be derived,

$$\begin{aligned}\mathbf{n}\times\tilde{\mathbf{H}}_{\rm T} &= \pm\frac{\gamma}{\mu_1}\left[\frac{1}{\gamma^2}{\rm i}\mathbf{k}_{\rm T}\left({\rm i}\mathbf{k}_{\rm T}\cdot\tilde{\mathbf{E}}_{\rm T}\right)+\tilde{\mathbf{E}}_{\rm T}\right], &(59)\\ \tilde{\mathbf{E}}_{\rm T}\times\mathbf{n} &= \pm\frac{\gamma}{\varepsilon_1}\left[\frac{1}{\gamma^2}{\rm i}\mathbf{k}_{\rm T}\left({\rm i}\mathbf{k}_{\rm T}\cdot\tilde{\mathbf{H}}_{\rm T}\right)+\tilde{\mathbf{H}}_{\rm T}\right]. &(60)\end{aligned}$$

These are used in conjunction with the wave field decomposition in Eq. (6) and the boundary condition in Eq. (4) or (5) to solve the impedance boundary value problem. After a lengthy derivation, the reflected electric and magnetic field strengths can be expressed in terms of the incident electric and magnetic field strengths, i.e.,

$$\begin{aligned}\tilde{\mathbf{E}}_{\rm T}^{\rm ref} &= \tilde{R}_{\rm Y}\tilde{\mathbf{E}}_{\rm T}^{\rm inc}-\frac{2}{\Delta_{\rm Y}\Delta_{\rm Z}}c_1\mathbf{k}_{\rm T}(c_1\mathbf{k}_{\rm T}\cdot\tilde{\mathbf{E}}_{\rm T}^{\rm inc}), &(61)\\ \tilde{\mathbf{H}}_{\rm T}^{\rm ref} &= \tilde{R}_{\rm Z}\tilde{\mathbf{H}}_{\rm T}^{\rm inc}-\frac{2}{\Delta_{\rm Y}\Delta_{\rm Z}}c_1\mathbf{k}_{\rm T}(c_1\mathbf{k}_{\rm T}\cdot\tilde{\mathbf{H}}_{\rm T}^{\rm inc}). &(62)\end{aligned}$$

In these expressions,

$$\begin{aligned}\tilde{R}_{\rm Y}(\gamma,s) &= 1-2\hat{Y}_{\rm n}/\Delta_{\rm Y}, &(63)\\ \tilde{R}_{\rm Z}(\gamma,s) &= 1-2\hat{Z}_{\rm n}/\Delta_{\rm Z}, &(64)\end{aligned}$$

are s-dependent reflection coefficients, in which

$$\Delta_{\rm Y}(\gamma,s)=\hat{Y}_{\rm n}(s)+c_1\gamma,\quad \Delta_{\rm Z}(\gamma,s)=\hat{Z}_{\rm n}(s)+c_1\gamma, \tag{65}$$

are denominator functions. The normal component of the reflected wave is obtained from the transform-domain compatibility relations, viz.,

$$\tilde{E}_z^{\rm ref}=-\gamma^{-1}{\rm i}\mathbf{k}_{\rm T}\cdot\tilde{\mathbf{E}}_{\rm T}^{\rm ref},\quad \tilde{H}_z^{\rm ref}=-\gamma^{-1}{\rm i}\mathbf{k}_{\rm T}\cdot\tilde{\mathbf{H}}_{\rm T}^{\rm ref}. \tag{66}$$

Equations (61)-(66) complete the slowness-domain solutions for the reflected wave fields in the elementary half-space configuration. Appendix B reviews the incident wave fields.

B. Space-time incident wave fields

Let $R_0(\mathbf{r})=(x^2+y^2+|z-h|^2)^{1/2}>0$ denote the distance between source and receiver, and $T^{\rm inc}(\mathbf{r})=R_0(\mathbf{r})/c_1$ the arrival time of the incident wave. Let

$$\mathcal{G}^{\rm inc}(\mathbf{r},t)=\frac{1}{4\pi R_0}H[t-T^{\rm inc}(\mathbf{r})], \tag{67}$$

denote the incident-wave Green's function. Then, the space-time incident EM wave fields generated by an electric dipole with orientation in the x-direction can be derived easily, e.g., via Eqs. (51)-(52), and are given by

$$\begin{aligned}E_x^{\rm inc}(\mathbf{r},t) &= \varepsilon_1^{-1}J(t)\overset{(t)}{*}\partial_x^2\mathcal{G}^{\rm inc}(\mathbf{r},t) &(68)\\ &\quad -\mu_1\partial_t^2J(t)\overset{(t)}{*}\mathcal{G}^{\rm inc}(\mathbf{r},t),\\ E_y^{\rm inc}(\mathbf{r},t) &= \varepsilon_1^{-1}J(t)\overset{(t)}{*}\partial_y\partial_x\mathcal{G}^{\rm inc}(\mathbf{r},t), &(69)\\ E_z^{\rm inc}(\mathbf{r},t) &= \varepsilon_1^{-1}J(t)\overset{(t)}{*}\partial_z\partial_x\mathcal{G}^{\rm inc}(\mathbf{r},t), &(70)\\ H_x^{\rm inc}(\mathbf{r},t) &= 0, &(71)\\ H_y^{\rm inc}(\mathbf{r},t) &= \partial_tJ(t)\overset{(t)}{*}\partial_z\mathcal{G}^{\rm inc}(\mathbf{r},t), &(72)\\ H_z^{\rm inc}(\mathbf{r},t) &= -\partial_tJ(t)\overset{(t)}{*}\partial_y\mathcal{G}^{\rm inc}(\mathbf{r},t). &(73)\end{aligned}$$

The slowness-domain counterparts of these expressions are substituted in Eqs. (61) and (62) to arrive at the slowness-domain reflected wave fields in Eqs. (10)-(15).

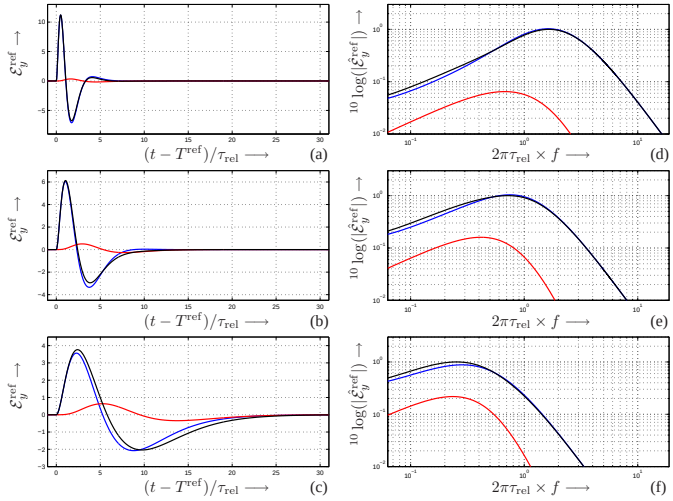

Fig. 3. Same as Fig. 2, but now for sea water as the second medium ($\varepsilon_2=81\varepsilon_0$, $\sigma_2=4.8$ Sm^{-1} and $\tau_{\rm rel}=1.50\times10^{-10}$ s).

C. Special case of a perfectly reflecting impedance wall

For the special cases $\sigma_2\rightarrow\infty$ and $\varepsilon_2\rightarrow\infty$, the impedance wall is perfectly reflecting. In both cases, $\hat{Y}_{\rm n}(s)\rightarrow\infty$ and $\hat{Z}_{\rm n}(s)\rightarrow0$, with the result that $\tilde{R}_{\rm Y}=-1$, $\tilde{R}_{\rm Z}=1$, and

$(\Delta_{\rm Y}\Delta_{\rm Y})^{-1}=0$. The solutions in Eqs. (10)-(15) become

$$E_x^{\rm ref,PR}(\mathbf{r},t) = -\varepsilon_1^{-1}J(t)\overset{(t)}{*}\partial_x^2\mathcal{G}^{\rm ref,PR}(\mathbf{r},t) +\mu_1\partial_t^2 J(t)\overset{(t)}{*}\mathcal{G}^{\rm ref,PR}(\mathbf{r},t), \quad (74)$$

$$E_y^{\rm ref,PR}(\mathbf{r},t) = -\varepsilon_1^{-1}J(t)\overset{(t)}{*}\partial_y\partial_x\mathcal{G}^{\rm ref,PR}(\mathbf{r},t), \quad (75)$$

$$E_z^{\rm ref,PR}(\mathbf{r},t) = -\varepsilon_1^{-1}J(t)\overset{(t)}{*}\partial_z\partial_x\mathcal{G}^{\rm ref,PR}(\mathbf{r},t), \quad (76)$$

$$H_x^{\rm ref,PR}(\mathbf{r},t) = 0, \quad (77)$$

$$H_y^{\rm ref,PR}(\mathbf{r},t) = \partial_t J(t)\overset{(t)}{*}\partial_z\mathcal{G}^{\rm ref,PR}(\mathbf{r},t), \quad (78)$$

$$H_z^{\rm ref,PR}(\mathbf{r},t) = -\partial_t J(t)\overset{(t)}{*}\partial_y\mathcal{G}^{\rm ref,PR}(\mathbf{r},t), \quad (79)$$

in which $\mathcal{G}^{\rm ref,PR}(\mathbf{r},t)=H(t-T^{\rm ref})/4\pi R_1$. Using the results of Appendix D in [27], it can be shown that these expressions are (apart from minus sign difference for the electric field strength) the solutions for the wave fields in homogeneous media. The latter was expected since the impedance wall was assumed perfectly reflecting. This shows that Eqs. (10)-(15) are consistent with the solutions for this special case.

D. Transformation back to the time domain

With the help of Eq. (17), Eq. (27) is rewritten as

$$\hat{K}_{\rm Y}(v,s)=\exp\left[-v\hat{X}_{\rm Y}^{1/2}(s)\right]. \quad (80)$$

Next, the Schouten-Van der Pol theorem (c.f. Formula 29.3.82 in [37]) is invoked to express the r.h.s. of Eq. (80) as an integral representation. This yields

$$\exp\left[-v\hat{X}_{\rm Y}^{1/2}(s)\right]=\int_{w=0}^{\infty}\Psi(v,w)\exp\left[-w\hat{X}_{\rm Y}(s)\right]{\rm d}w, \quad (81)$$

in which

$$\Psi(v,w)=\frac{v}{(4\pi w^3)^{1/2}}\exp(-v^2/4w)H(w), \quad (82)$$

is the kernel function well-known from the theory of partial differential equations on diffusion processes [38]. The r.h.s. of Eq. (81) is now in an appropriate form for finding $K_{\rm Y}(v,t)$ analytically. The time-domain counterpart of $\hat{K}_{\rm Y}(v,s)$ is first expressed as

$$K_{\rm Y}(v,t) = \mathcal{L}^{-1}\left\{\exp\left[-v\hat{X}_{\rm Y}^{1/2}(s)\right]\right\}= \int_{w=0}^{\infty}\Psi(v,w)\exp\left(-F^2w\right)\mathcal{L}^{-1}\left\{\exp\left(-wF^2\tau_{\rm rel}^{-1}s^{-1}\right)\right\}{\rm d}w, \quad (83)$$

in which $\mathcal{L}^{-1}$ stands for the inverse Laplace transformation. With the aid of the identity (cf. Formula 29.3.75 in [37]),

$$s^{-1}\exp\left(-ks^{-1}\right) = \int_{t=0}^{\infty}\exp(-st)\left\{J_0\left[2(kt)^{1/2}\right]H(t)\right\}{\rm d}t, \quad k\geq 0, \quad (84)$$

$K_{\rm Y}(v,t)$ is explicitly found as

$$K_{\rm Y}(v,t) = \int_{w=0}^{\infty}\Psi(v,w)\left\{\exp(-F^2w)\delta(t)- F\exp(-F^2w)\left(\frac{w\tau_{\rm rel}^{-1}}{t}\right)^{1/2}J_1\left[2F(wt\tau_{\rm rel}^{-1})^{1/2}\right]H(t)\right\}{\rm d}w, \quad (85)$$

in which J_1 stands for the Bessel function of the first kind and order one.

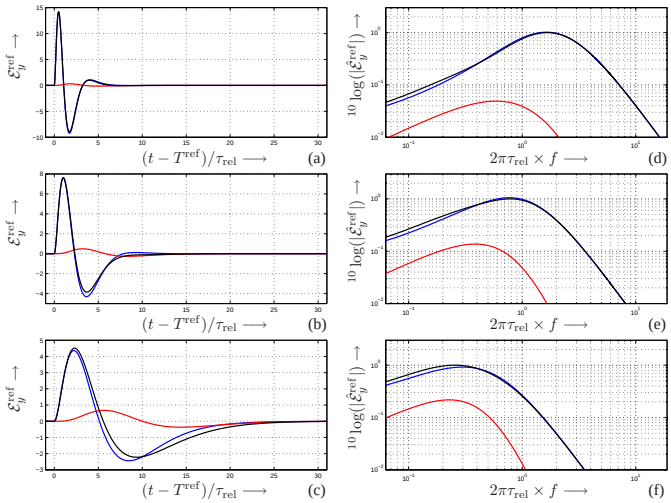

Fig. 4. Same as Fig. 2, but now for wet soil as the second medium ($\varepsilon_2=20\varepsilon_0$, $\sigma_2=0.1$ Sm^{-1} and $\tau_{\rm rel}=1.7708\times10^{-9}$ s).

E. Space-time reflected electric field strength corresponding to $\mathcal{G}_{\rm Z}^{\rm ref}$

The reflected electric field strength $E_y^{\rm ref}(\mathbf{r},t)$ corresponding to $\mathcal{G}_{\rm Z}^{\rm ref}(\mathbf{r},t)$ is reviewed. Similar to [27], $E_y^{\rm ref}$ is written as

$$E_y^{\rm ref}(\mathbf{r},t)=E_y^{{\rm ref},1}(\mathbf{r},t)+E_y^{{\rm ref},2}(\mathbf{r},t), \quad (86)$$

in which

$$E_y^{{\rm ref},1}(\mathbf{r},t) = \varepsilon_1^{-1}(T^{\rm ref})^2\partial_t J[t-T^{\rm ref}(\mathbf{r})]\mathcal{G}_{E_y}^{{\rm ref},1;{\rm FF}}(\mathbf{r}) +\varepsilon_1^{-1}T^{\rm ref}J[t-T^{\rm ref}(\mathbf{r})]\mathcal{G}_{E_y}^{{\rm ref},1;{\rm IF}}(\mathbf{r}) +\varepsilon_1^{-1}\int_{\tau=T^{\rm ref}}^{t}J(t-\tau)\mathcal{G}_{E_y}^{{\rm ref},1;{\rm NF}}(\mathbf{r},\tau){\rm d}\tau, \quad (87)$$

is the constant-admittance part of $E_y^{\rm ref}$, and

$$E_y^{{\rm ref},2}(\mathbf{r},t)=\varepsilon_1^{-1}\int_{\tau=T^{\rm ref}}^{t}J(t-\tau)\mathcal{G}_{E_y}^{{\rm ref},2;{\rm NF}}(\mathbf{r},\tau){\rm d}\tau, \quad (88)$$

represents the dispersive part of the total-admittance $E_y^{\rm ref}$. The RWGT components in Eqs. (87)-(88) are given by

$$\mathcal{G}_{E_y}^{{\rm ref},1;{\rm FF}}(\mathbf{r},t) = -\frac{xyG_{\rm Z}^{{\rm ref},1}[\mathbf{r},T^{\rm ref}(\mathbf{r})]}{R_1^4}H[t-T^{\rm ref}(\mathbf{r})], \quad (89)$$

$$\mathcal{G}_{E_y}^{{\rm ref},1;{\rm IF}}(\mathbf{r},t) = H[t-T^{\rm ref}(\mathbf{r})]\{\frac{x\partial_y G_{\rm Z}^{{\rm ref},1}[\mathbf{r},T^{\rm ref}(\mathbf{r})]}{R_1^2} -\frac{xyG_{\rm Z}^{{\rm ref},1}[\mathbf{r},T^{\rm ref}(\mathbf{r})]}{R_1^4}+\frac{y\partial_x G_{\rm Z}^{{\rm ref},1}[\mathbf{r},T^{\rm ref}(\mathbf{r})]}{D_1^2}\}, \quad (90)$$

$$\mathcal{G}_{E_y}^{{\rm ref},1;{\rm NF}}(\mathbf{r},t) = -\partial_x\partial_y G_{\rm Z}^{{\rm ref},1}(\mathbf{r},t)H[t-T^{\rm ref}(\mathbf{r})], \quad (91)$$

$$\mathcal{G}_{E_y}^{{\rm ref},2;{\rm NF}}(\mathbf{r},t) = -\partial_x\partial_y G_{\rm Z}^{{\rm ref},2}(\mathbf{r},t)H[t-T^{\rm ref}(\mathbf{r})], \quad (92)$$

in which the first two terms represent the far- and intermediate-zone contributions, respectively, whereas the last two terms represent the near-zone contributions to $E_y^{\rm ref}$. The following identity, cf. [27], is easily obtained

$$G_{\rm Z}^{{\rm ref},1}[\mathbf{r},T^{\rm ref}(\mathbf{r})]=\frac{1}{4\pi R_1}\left[1-\frac{2}{F\cos(\theta)+1}\right], \quad (93)$$

from which the expressions

$$\begin{aligned}
\partial_x G_{\mathrm{Z}}^{\mathrm{ref},1}[\mathbf{r}, T^{\mathrm{ref}}(\mathbf{r})] &= \frac{x}{4\pi R_1^3}\left\{\frac{2}{[F\cos(\theta)+1]^2}-1\right\},\\
\partial_y G_{\mathrm{Z}}^{\mathrm{ref},1}[\mathbf{r}, T^{\mathrm{ref}}(\mathbf{r})] &= \frac{y}{4\pi R_1^3}\left\{\frac{2}{[F\cos(\theta)+1]^2}-1\right\},\\
\partial_z G_{\mathrm{Z}}^{\mathrm{ref},1}[\mathbf{r}, T^{\mathrm{ref}}(\mathbf{r})] &= \\
&\frac{F+\cos(\theta)}{2\pi R_1^2[F\cos(\theta)+1]^2}-\frac{\cos(\theta)}{4\pi R_1^2},
\end{aligned} \tag{94}$$

are derived.

REFERENCES

[1] M. A. Leontovich, "Methods of solution for problems of electromagnetic waves propagation along the Earth surface," *Bull. Acad. Sci. USSR, Phys. Ser.*, vol. 8, no. 1, p 1622, 1944, (in Russian).

[2] A. N. Shchukin, *Propagation of Radio Waves*. Moscow, Russia: Svyaz-izdat, 1940.

[3] S. W. Lee and W. Gee, "How good is the impedance boundary condition?," *IEEE Trans. Antennas Propag.*, vol. 35, no. 11, pp. 1313-1315, 1987.

[4] D. J. Hoppe and Y. Rahmat-Samii, *Impedance Boundary Conditions in Electromagnetics*. Washington, DC: Taylor & Francis, 1995.

[5] I. V. Lindell and A. H. Sihvola, "Realization of impedance boundary," *IEEE Trans. Antennas Propag.*, vol. 54, no. 12, pp. 3669-3676, 2006.

[6] A. Karlsson, "Approximate boundary conditions for thin structures," *IEEE Trans. Antennas Propag.*, vol. 57, no. 1, pp. 144-148, 2009.

[7] J. Jin, *The Finite Element Method in Electromagnetics*. Wiley-IEEE Press, 2nd ed., 2002.

[8] A. Taflove and S. C. Hagness, *Computational Electrodynamics: The Finite-Difference Time-Domain Method*. Artech House Publishers, 3rd ed., 2005.

[9] K. S. Oh and J. E. Schutt-Aine, "An efficient implementation of surface impedance boundary conditions for the finite-difference time-domain method," *IEEE Trans. Antennas Propag.*, vol. 43, no. 7, pp. 660-666, 1995.

[10] D. V. Thiel and R. Mittra, "Surface impedance modelling using the finite-difference time-domain method," *IEEE Trans. Geosci. Remote Sens.*, vol. 35, no. 5, pp. 1350-1356, 1997.

[11] R. F. Harrington and J. R. Mautz, "An impedance sheet approximation for thin dielectric shells," *IEEE Trans. Antennas Propag.*, vol. 23, no. 7, pp. 531-534, 1975.

[12] R. J. Luebbers and K. Kunz, "FDTD modelling of thin impedance sheets," *IEEE Trans. Antennas Propag.*, vol. 40, pp. 349-351, 1992.

[13] T. B. Senior, "Approximate boundary conditions," *IEEE Trans. Antennas and Propag.*, vol. 29, pp. 826-829, 1981.

[14] S. van den Berghe, F. Olyslager, and D. de Zutter, "Accurate modelling of thin conducting layers in FDTD," *IEEE Microw. Guided Wave Lett.*, vol. 8, no. 2, pp. 75-77, 1998.

[15] J. C. Rautio and V. Demir, "Microstrip conductor loss models for electromagnetic analysis," *IEEE Trans. Microwave Theory Tech.*, vol. 28, no. 3, pp. 434-444, 2005.

[16] M.-Y. Xia, C. H. Chan, and W. C. Chew, "Time-domain Green's functions for the microstrip structures using Cagniard-de Hoop method," *IEEE Trans. Antennas and Propag.*, vol. 52, no. 6, pp. 1578-1585, 2004.

[17] K. M. Coperich, A. E. Ruehli and A. C. Cangellaris, "Enhanced skin effect for partial-element equivalent-circuit (PEEC) models," *IEEE Trans. Microwave Theory Tech.*, vol. 48, no. 9, pp. 1435-1442, 2000.

[18] D. de Zutter, H. Rogier, L. Knockaert, and J. Sercu, "Surface current modelling of the skin effect for on-chip interconnects," *IEEE Trans. Adv. Pack.*, vol. 30, no. 2, pp. 342-349, 2007.

[19] A. Rong, A. C. Cangellaris, and L. Dong, "Comprehensive broadband electromagnetic modelling of on-chip interconnect with a surface discretization-based generalized PEEC model," *IEEE Trans. Adv. Pack.*, vol. 28, no. 3, pp. 434-444, 2005.

[20] I. V. Lindell and E. Alanen, "Exact image theory for the Sommerfel half-space problem, II, Vertical electric dipole," *IEEE Trans. Antennas Propag.*, vol. 32, no. x, pp. 841-847, 1984.

[21] B. J. Kooij, "The electromagnetic field emitted by a pulsed current point source above the interface of a nonperfectly conducting Earth," *Radio Science*, vol. 31, no. 6, pp. 1345-1360, 1996.

[22] R. W. P. King, M. Owens, and T. T. Wu, *Lateral Electromagnetic Waves, Theory and Applications to Communications*, Geophysical Exploration, and Remoting Sensing, Springer-Verlag, 1992.

[23] K. Li, *Electromagnetic Fields in Stratified Media*, Springer-Verlag, Berlin, Germany, 2009.

[24] H. J. Frankena,"Transient phenomena associated with Sommerfeld's horizontal dipole problem," *Appl. Sci. Res.*, vol. 8, pp. 357-368, 1960.

[25] R. W. P. King, "Lateral electromagnetic pulses generated on a plane boundary between dielectrics by vertical and horizontal dipole source with Gaussian pluse excitation," *J. Electrom. Waves Appl.*, vol. 2, pp. 589-597, 1989.

[26] A. T. de Hoop, "Transient diffusive electromagnetic fields in stratified media - Calculation of the two-dimensional E-polarized field," *Radio Science*, vol. 35, pp. 443-453, 2000.

[27] M. C. H. Lam, "Impulsive radiation from a vertical electric dipole above an imperfectly conducting surface," *accepted in IEEE Trans. Antennas Propag.*, 2012.

[28] A. T. de Hoop and H. J. Frankena, "Radiation of pulses generated by a vertical electric dipole above a plane, nonconducting, Earth," *Appl. Sci. Res., Sect. B*, vol. 8, pp. 369-377, 1960.

[29] C. H. Lam, B. J. Kooij, and A. T. de Hoop, "Impulsive sound reflection from an absorptive and dispersive planar boundary," *J. Acoust. Soc. Am.*, vol. 116, no. 2, pp. 677-685, 2004.

[30] A. T. de Hoop, C. H. Lam and B. J. Kooij, "Parametrization of acoustic boundary absorption and dispersion properties in time-domain source/receiver reflection measurement," *J. Acoust. Soc. Am.*, vol. 118, no. 2, pp. 654-660, 2005.

[31] D. V. Widder, *The Laplace Transform*. New Jersey: Princeton University Press, pp. 61-63, 1946.

[32] J. P. Schouten "A new theorem in operational calculus together with an application of it," *Physica* (Amsterdam), 1, pp. 75-80, 1934.

[33] B. van der Pol, "A theorem on electrical networks with applications to filters," *Physica* (Amsterdam), 1, pp. 521-530, 1934.

[34] B. van der Pol and H. Bremmer *Operational Calculus Based on the Two-sided Laplace Transform*. Cambridge University Press, Cambridge, UK, pp. 232-236, 1950.

[35] J. P. Schouten, *Operatorenrechnung*. Springer, Berlin, pp. 124-126, 1961.

[36] Kay and Laby, Tables of physical & chemical constants. Online: http://www.kayelaby.npl.co.uk/general_physics/2_7/v2_7_9.html

[37] M. Abramowitz and I. A. Stegun, *Handbook of Mathematical Functions*. Dover Publications, Inc., New York, USA, p 1020, 1972.

[38] W. A. Strauss, *Partial Differential Equations: An Introduction*. John Wiley & Sons, Inc., New York, USA, Sect. 2.3, 1992.